



Laminated collagen-fiber bio-composites for soft-tissue bio-mimetics



Mirit Sharabi ^{a, b}, Dafna Benayahu ^b, Yehuda Benayahu ^c, Jessica Isaacs ^d, Rami Haj-Ali ^{a, *}

^a School of Mechanical Engineering, The Fleischman Faculty of Engineering, Tel Aviv University, Tel Aviv 69978, Israel

^b Department of Cell and Developmental Biology, Sackler School of Medicine, Tel Aviv University, Tel Aviv 69978, Israel

^c Department of Zoology, George S. Wise Faculty of Life Sciences, Tel Aviv University, Tel Aviv 69978, Israel

^d Department of Mechanical Engineering, Widener University, Chester, PA 19013, USA

ARTICLE INFO

Article history:

Received 29 March 2015

Received in revised form

24 June 2015

Accepted 28 June 2015

Available online 8 July 2015

Keywords:

Laminate

Fiber

Non-linear behavior

Modelling

Bio-composite

ABSTRACT

The objective of this study was to introduce a class of collagen-fiber reinforced bio-composite laminates as biomimetic of soft tissues. These novel all-natural bio-composite laminates include long collagen fibers from soft coral embedded in an alginate hydrogel matrix. Controlling the fiber orientation and volume fraction enabled the fabrication of laminates with wide range of mechanical behaviors. Four material systems were investigated in the current study having different fiber orientations: longitudinal (0°), transverse (90°), cross-ply ($0/90^\circ$) and angle-ply ($\pm 30^\circ$). The range of Fiber volume fractions (FVFs) for the laminated membranes is between 0.21 and 0.31. The laminates were subjected to uniaxial loading, yielding hyperelastic stress-strain behavior.

A hyperelastic finite element (FE) model was constructed for the heterogeneous laminate, based on the fiber and matrix hyperelastic material behavior and their FVF, in order to predict the overall bio-composite mechanical behavior. The predictions of the FE model were verified from the tested laminated systems. The FE model consisted of beam elements representing the collagen fibers embedded in the solid matrix (alginate). Good predictions were demonstrated by the proposed FE model compared with the tested bio-composites for all orientations up to 10% strain. The overall hyperelastic stress-strain behavior was in a similar range to known native soft tissues. In addition, the model allowed for examining the mechanical behavior of laminates with other FVFs. The new bio-composite material can be used for future soft tissue mimicry and repair.

© 2015 Elsevier Ltd. All rights reserved.

1. Introduction

Thin layers with oriented collagen fibers are the principal building blocks of many soft tissues [1–4]. Nature, in its thousands of years of evolution, has created a variety of specialized collagen-based heterogeneous tissues based on the same repeating building blocks. The variations in composition, orientation and distribution of fibers are responsible for a wide range of distinct mechanical behaviors. Yet, soft tissues share the similar overall hyperelastic behavior due to collagen's hierarchical structure [1].

The desire to mimic these natural structures has driven biomechanical engineers to develop custom-made bio-inspired materials with mechanical properties similar to natural tissues. New biomaterials are constantly being designed to function in extremely complicated physiological surroundings [5–8].

Biomimetics of shape and form of tissue structures is still in its infancy, however, complex structures of biomaterials as cartilage [9], anterior cruciate ligament [10], blood vessels [11] and annulus fibrosus [12] are designed as the tissue itself. Specific structural characteristics as nanofibers net [2,13], fiber crimping [14,15] and fiber orientations [12,16] are being developed towards creation of suitable tissue analogs. Currently, the preferred biomaterials are the native tissues themselves [17]. Mimicking the hyperelastic behavior of native tissues is essential to prevent regional mismatch while a new graft is assimilated to the host tissue. This discrepancy can induce local stress concentration due to stiffness mismatch between the native tissue and the implanted graft, which can result in hyperplasia or even tissue failure [18].

Mechanical properties of biomaterials can be tuned by adjusting diverse parameters, such as crosslinking [19], material concentration [20,21], and architecture [22,23]. The mechanical properties of fiber-reinforced bio-composites are relatively easier to manipulate by adjusting their fiber fraction and orientation. Scaffolds based on bio-composites have been designed for blood vessels [11],

* Corresponding author.

E-mail address: rami98@tau.ac.il (R. Haj-Ali).

abdominal walls [24], cartilage [25], and cardiac tissue [26], combine mechanical robustness with biological functioning similar to native tissue structures.

Computational simulations for the mechanical behavior of newly engineered biomaterials may lead to rapid progress and accelerate their development. Such computational models have the potential to design and introduce new biomaterial systems and to simulate their response to multiaxial loadings in order to obtain optimized materials and structures. For example, Sasson et al. [27] have examined the hyperelastic behavior of chitosan gel for nucleus pulposus replacement using hyperelastic constitutive FE model to test other loading modes. Neal et al. [28] have simulated the mechanical properties of poly(glycerol sebacate) (PGS) scaffold in different patterns in order to design desirable material properties for cardiac tissue scaffold. Pore fraction influence was tested using hyperelastic Neo–Hookean material model to simulate the non-linear behavior of PGS [29]. Fabrication and mechanical testing of oriented electrospun fiber laminates seeded with annulus fibrosus cells with a combination of *in silico* anisotropic constitutive model were developed [13,30,31]. The mechanical behavior of the anisotropic laminates was examined and the influence of fiber orientation, interlamellar interactions and tissue growth were explored.

Our previous study [32,33] presented a new natural collagen-fiber-reinforced alginate hydrogel matrix with limited mechanical characterization focusing on a unidirectional fiber alignment. In this paper, we expand the mechanical characterizations and modeling of both unidirectional and multi-oriented laminated bio-composites using controlled fiber fractions and orientations that ultimately can mimic soft tissues. The unique long collagen fibers are derived from soft coral, consisting of natural coiling, and comprising a high degree of crosslinking and *in vivo* biocompatibility. The new material system is fabricated as a set of laminates each with different fiber orientation. Fiber orientation and volume fraction are controlled and can be manipulated to produce different overall hyperelastic mechanical behaviors. Four 3D FE analyses are generated for the heterogeneous laminates, calibrated for their fiber and matrix constituents, and validated to examine their ability to predict the tested mechanical behavior of the proposed bio-composite material systems.

2. Materials and methods

2.1. Bio-composite fabrication and material characterization

2.1.1. Isolation and purification of coral collagen fibers

Soft coral sarcophyton sp. colonies were stored in 70% ethanol. A piece of coral was harvested and the collagen fibers were exposed by reaping the edge of the coral. The reaping of the coral opens its mesenteries which in the fibers are found and highly coiled [34]. While the pieces of the coral move apart, the coiled fibers are straightened and exposed, allowing their further arrangement in the composite. The fibers are organized in the collagen in a nested hierarchical structure and their bundle diameter when extracted was ranged $61.5 \pm 14.3 \mu\text{m}$. The extracted fibers were then wrapped around thin stainless steel frames to create parallel, organized fiber arrays. Four different orientations were fabricated: unidirectional-longitudinal (0°), transverse (90°), cross-ply (fibers wrapped at 0° and 90°) and angle-ply (fibers wrapped at 60° angles). The orientations were determined by each frame geometry: U-shaped for transverse and longitudinal, rectangular for cross-ply and hexagonal for angle-ply. Angle-ply orientations were created by spinning the fibers first in one direction and then in the second. The reinforced collagen fibers were washed with ethanol (70% v/v) and double-distilled water (DDW).

2.1.2. Fabrication

The arrayed collagen fiber frames were inserted into a dialysis membrane (6000–8000 MWCO, Spectra Por, SpectrumLabs, USA) with a 3% w/v sodium alginate solution (Protanal LF 10-60, FMC biopolymer, USA) in DDW and were cross-linked with 45 mM EDC/NHS (N-(3-Dimethylaminopropyl)-N'-ethylcarbodiimide hydrochloride, Sigma–Aldrich, Israel)/(N-Hydroxysuccinimide, Sigma–Aldrich, Israel). The dialysis membrane was sealed, flattened and soaked in a 0.1 M CaCl_2 (Merck, USA) solution for 48 h at room temperature to enable ionic gelation of the alginate hydrogel through diffusion. The complete bio-composite was then removed from the membrane and frame.

2.1.3. Fiber orientation and characterization

Images of the reinforced fibers were taken with a digital microscope (AM311S, BigCatch, Taiwan) on a dark background. The images were processed into binary numerical arrays, followed by calculating the percentage of white pixels (representing the fibers) that stood out against the dark background to determine the fiber fraction. Image processing and calculations were conducted using a computational program (Matlab). The fraction was normalized to the final bio-composite thickness. Fiber orientation was captured using the OrientationJ (Biomedical Imaging Group, École Polytechnique Fédérale de Lausanne, Switzerland) plugin to the ImageJ (NIH) software [35].

2.1.4. Scanning electron microscopy

Collagen fiber microstructural feature examination was conducted by scanning electron microscope (SEM) (Quanta 200 FEG Environmental Scanning Electron Microscope). The samples were fixed in 4% formaldehyde and dehydrated through a series of graded ethanol agents, from 70% to 100% concentration. The samples were sputtered with a gold–palladium alloy and then examined with a SEM under high-vacuum conditions.

2.2. Mechanical testing

Tensile testing was performed using an Instron – 5582 loading frame with a 100 N load cell at a rate of 0.05 mm s^{-1} . Samples were preconditioned and then stretched to failure. Longitudinal samples were stretched parallel to the fiber, at an angle of 0° between the fibers and the loading direction. Transverse bio-composites were stretched perpendicular to the fiber direction. Cross-ply laminates were stretched with one ply in the tensile direction and the other perpendicular to the tensile direction ($0^\circ/90^\circ$). Angle-ply laminates, which were fabricated with 60° between fiber plies, were stretched to create a $\pm 30^\circ$ angle with the tensile axis.

Means and standard deviations (SD) were calculated for all measurements. Results with values of $p < 0.05$ were considered statistically significant.

2.3. Finite element analysis

A finite element (FE) model was constructed to simulate the mechanical behavior of the fabricated laminates using the Abaqus FE software (Dassault Systems, Simulia Corp., Providence, RI, USA). The model was composed of heterogeneous 3D rectangular-shaped plate, similar to the fabricated bio-composites. The plate was constructed with solid elements, represented the alginate matrix. Beam elements representing the collagen were attached between the solid elements' nodes (beam type B31H elements and solid C3D8H elements). Therefore, for each two-noded beam element, shared common nodes were used with the matched solid element to allow for translation-only kinematic constraint and its associates load transfer between the matrix and the collagen constituents.

Hybrid solid elements were used due to the incompressible nature of biological materials. Furthermore, validation of the nearly incompressible material behavior was done using confined and unconfined compression tests [27]. The fiber volume fraction was equivalent to the mean experimental fraction as shown in Table 1. The detailed problem size in terms of node and element numbers are listed in Table 2. The materials' stress–strain behavior, shown in Fig. 1, were both considered hyperelastic; the same material properties were used for all four analyzed cases. The collagen's effective hyperelastic mechanical behavior was calibrated to fit the overall behavior based on experimental data, which was fitted using an Ogden strain energy density function (order 3) [36] as presented in Eq. (1). A Marlow hyperelastic model [37,38] was used for the alginate matrix that was considered to be homogenous and isotropic and presented in Eq. (2). The volumetric part of the equations was neglected due to the nearly incompressible nature of the bio-composite.

$$U = \sum_{i=1}^{N=3} \frac{2\mu_i}{\alpha_i^2} (\bar{\lambda}_1^{\alpha_i} + \bar{\lambda}_2^{\alpha_i} + \bar{\lambda}_3^{\alpha_i} - 3) + \sum_{i=1}^{N=3} \frac{1}{D_i} (J_{el} - 1)^{2i} \quad (1)$$

$$U = U_{dev}(\bar{\lambda}_1 + \bar{\lambda}_2 + \bar{\lambda}_3) + U_{vol}(J_{el}) \quad (2)$$

The matrix stress–strain behavior was taken from the matrix-alone tensile measurements. The FE model employed implicit nonlinear dynamic analysis. The boundary conditions matched the mechanical tested samples for supported plate under uniaxial load subjected through displacement control. The influence of off-axis fibers was tested on the longitudinal and transverse composites, by deviation of the fibers in 2-degrees in the longitudinal and transverse models while gradually increasing the FVFs from 1.25% to 6.5%.

3. Results

The fabrication process created consistent bio-composites of long coral collagen fibers embedded in alginate hydrogel matrices with four fiber orientation formats: unidirectional (longitudinal and transverse), cross-plied and angle-plied, as shown in Fig. 2.

The laminates' geometrical properties are listed in Table 1. The fiber orientations were arranged according to each frame geometry (0°, 90°, 0°/90° and ±30° with the vertical axis). The orientation angles were verified using OrientationJ, as evident in Fig. 3. SEM images of the aligned fibers confirmed that the collagen fibers retained their coiled structure post-processing and alignment (Fig. 4a). Variations in orientation in each group were not substantial as seen in the representative OrientationJ-generated colormap (Fig. 3 and Table 1), although there were off-axis fibers detected by SEM as observed in Fig. 4b,c.

The mechanical behavior of the bio-composite materials were examined under tensile loading using a mechanical testing setup, as shown in Fig. 2a.

The general behavior of all laminates was hyperelastic with large deformations; the laminates demonstrated non-linear

Table 2
Finite element model size and material parameters for matrix and fibers.

Model	Nodes	Elements	Degrees of freedom (DOF)
Longitudinal	88,564	56,564	311,764
Transverse	88,564	56,564	311,764
Cross-plied	88,564	56,564	311,290
Angle-plied	71,809	40,209	214,101

Material parameters			
	Ogden order 3-fibers	Marlow-tabular uniaxial data (matrix)	
		Strain[mm/mm]	Stress [MPa]
μ1	−353.23	0.000	0.000
		0.020	0.002
		0.049	0.020
α1	−13.53	0.058	0.030
		0.077	0.051
		0.086	0.062
μ2	205.77	0.095	0.073
		0.104	0.082
		0.113	0.090
α2	−10.13	0.113	0.090
		0.122	0.096
		0.131	0.104
μ3	148.17	0.140	0.109
		0.148	0.116
		0.148	0.116

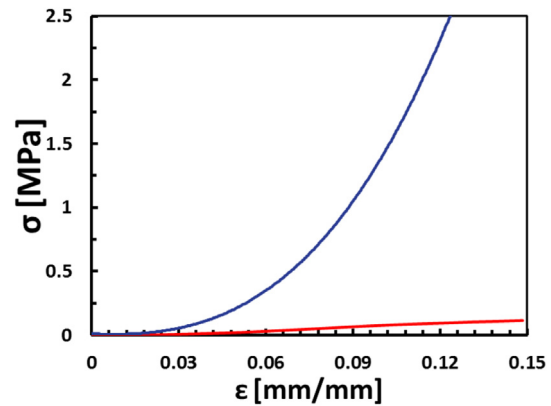


Fig. 1. Hyperelastic true stress–strain response used in the FE models.

stress–strain relationships (Fig. 6). The mechanical measurements are presented as the true (Cauchy) stress and logarithmic strain values. The ultimate tensile strength (UTS) was taken as the maximum stress before failure and measured to be 0.68 ± 0.34 MPa and the ultimate strain was taken as the maximum strain before failure was measured to be 0.20 ± 0.04 . The mechanical properties of each tested group are shown in Table 1. The mean fiber fraction was $24 \pm 9\%$, the differences among the groups were not statistically significant (Fig. 5a, p-value = 0.1073). Therefore, the groups could be compared, although cross-plied bio-composites presented a slightly higher average fiber fraction, which probably had an effect on the tensile strength. A significant difference was seen in the

Table 1
Geometrical and mechanical properties of bio-composites.

Orientation (nominal angle)	n	Thickness [mm]	Width [mm]	Length [mm]	Fiber fraction	Variation around nominal angle [°] ^a	Ultimate tensile strain [mm/mm]	Ultimate tensile strength [MPa]
Longitudinal (0°)	8	0.62 ± 0.13	9.8 ± 2.3	25.2 ± 4.3	0.21 ± 0.07	-1.5 ± 0.69	0.17 ± 0.02	0.75 ± 0.21
Transverse (90°)	6	0.71 ± 0.14	11.8 ± 1.0	17.5 ± 3.5	0.22 ± 0.05	89.2 ± 2.23	0.21 ± 0.05	0.29 ± 0.13
Cross-plied (90°)	7	0.60 ± 0.26	12.3 ± 1.9	22.7 ± 5.0	0.31 ± 0.13	90.7 ± 4.69	0.20 ± 0.01	0.99 ± 0.32
Angle-plied (60°)	6	0.8 ± 0.19	10.5 ± 1.0	17.9 ± 3.2	0.21 ± 0.06	58.0 ± 8.77	0.23 ± 0.03	0.64 ± 0.31

^a The measured angle was the angle with the vertical axis for the unidirectional orientations and between the plies for the plied orientations.

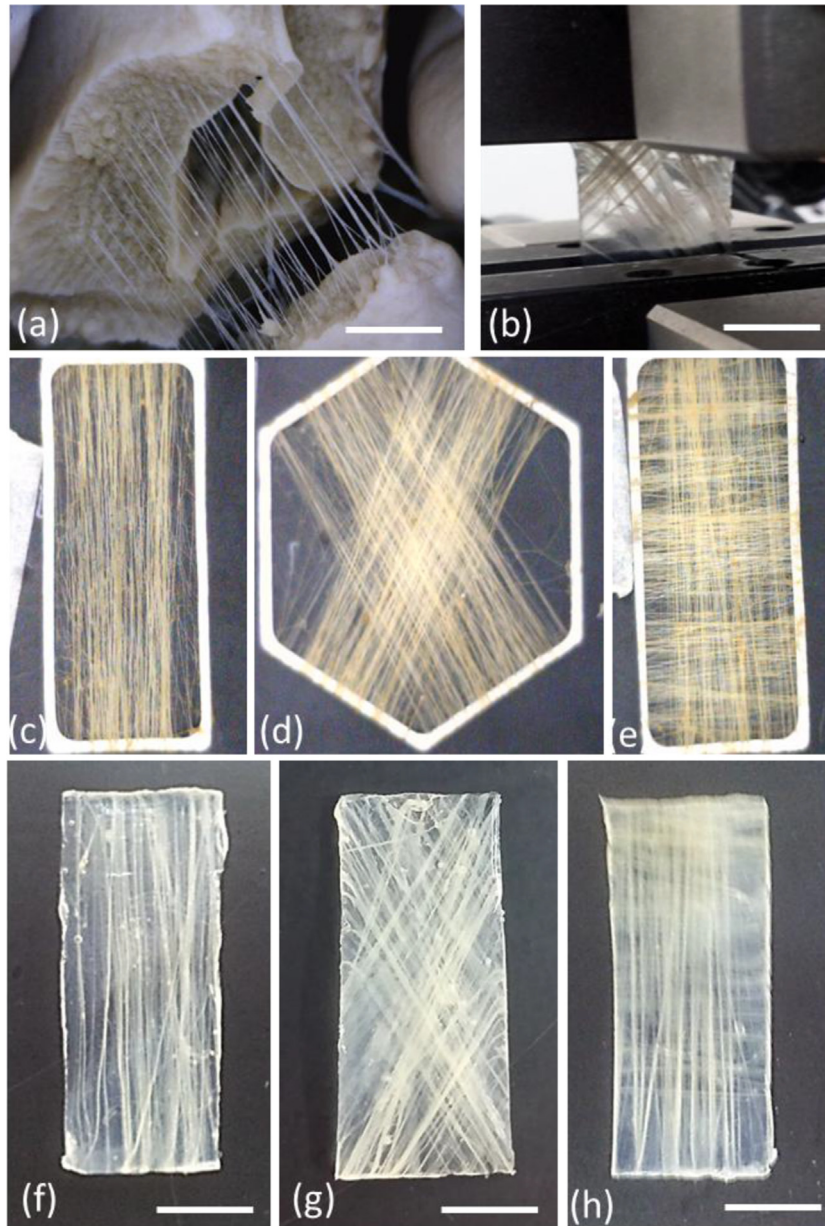


Fig. 2. Collagen-alginate bio-composites: (a) Extraction of collagen fibers from soft coral. (b) Tensile test of an angle-ply bio-composite. (c–e) Three collagen fiber alignments: longitudinal, angle-ply and cross-ply, respectively. (f–h) Different bio-composite orientations: longitudinal, angle-ply and cross-ply, respectively (Scale bars in white are 10 mm).

ultimate strains of the angle-ply and longitudinal groups ($p = 0.0059$), as demonstrated in Fig. 5b. Ultimate tensile strength was significantly higher in the longitudinal samples and cross-ply samples in comparison to the transverse samples (0.75 ± 0.21 MPa, 0.99 ± 0.32 MPa and 0.29 ± 0.13 MPa, respectively). The laminates' effective stress–strain behaviors are presented in Fig. 6 as means and standard deviation.

Three-dimensional FE models were generated to simulate the mechanical response of the bio-composite laminates having the same fiber fraction. A strain rate of 1 mm s^{-1} was used for all FE models. When all the fibers were aligned in the loading direction, the bio-composite axial stress at 18% strain was about 3 orders of magnitude higher than the matrix, and when the fibers were orthogonal to the loading direction, their influence was negligible (Fig. 6). The experimental fiber volume fraction was not identical in

all samples; therefore, the cross-ply model was recalculated with a compatible fiber fraction of 21%, the same as the other laminates, to allow a better comparison between the models. The influence of off-axis fiber deviation was very small (Fig. 6A,B) in the longitudinal and transverse models, therefore the use of the FE models with the major direction is proven accurate.

Fig. 7 summarizes the results of the four oriented composite models for the same fiber volume fraction. It shows that the longitudinal composite was stiffer than the cross-ply, which was stiffer than the angle-ply ($\pm 30^\circ$). These three composites were stiffer than the transverse laminate, as expected.

The strain rate influence on mechanical behavior was examined in the FE models. The difference between the experimental rate and the computational rate was negligible, with a minor difference of 1.8%, allowing the use of a faster strain rate to enhance

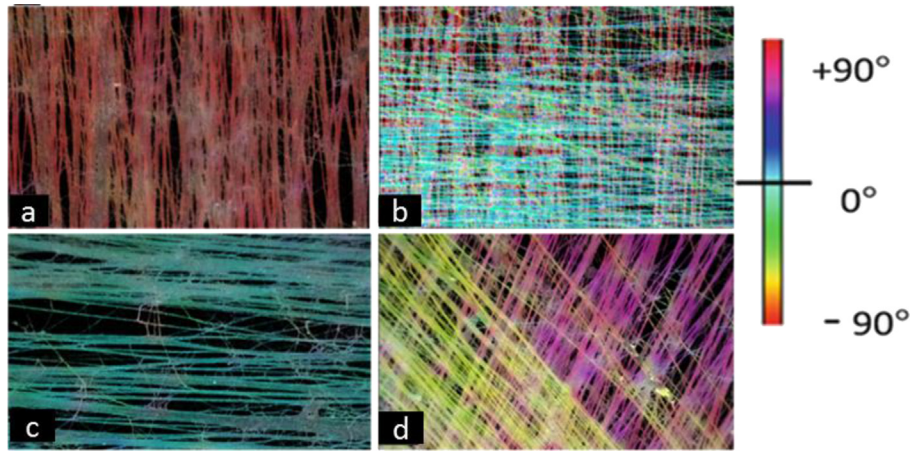


Fig. 3. Fiber orientation characterization using the OrientationJ plugin (ImageJ, NIH). (a) Longitudinal. (b) Cross-plyed. (c) Transverse. (d) Angle-plyed. The color map represents the angle with the horizontal axis. (For interpretation of the references to colour in this figure legend, the reader is referred to the web version of this article.)

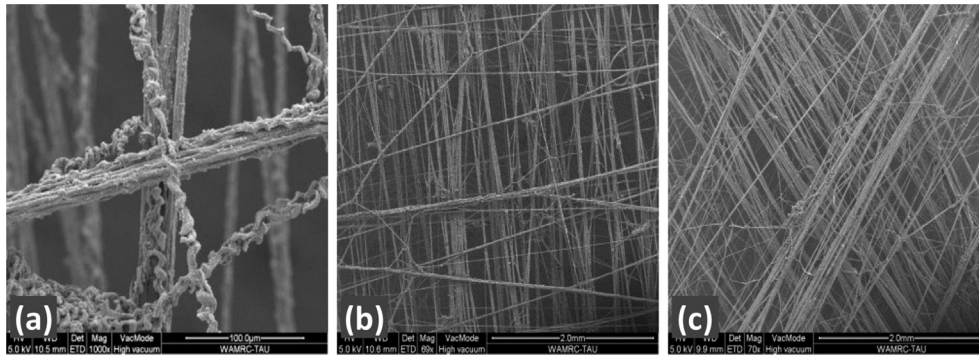


Fig. 4. SEM images of isolated collagen fibers. (a, b) Cross-plyed fibers (magnifications of $\times 1000$ and $\times 69$, respectively). (c) Angle-plyed fibers (magnification of $\times 70$).

computational efficiency and convergence.

The proposed FE model and its numerical predictions are in good agreement with the experimental results up to 10% strain (Fig. 6). The angle-plyed results showed a very good fit throughout the strain range, as demonstrated in Fig. 6D. Longitudinal and cross-plyed laminates presented very close response up to 10% strain, as seen in Fig. 6A,C. The predictions for the transverse laminate stress levels were slightly lower than the experimental values, but higher than the matrix-alone, as demonstrated in Fig. 6B. The simultaneous use of the same material properties in all tested fiber orientations verified the numerical results.

The FE models allowed examining the mechanical response of

laminates for additional fiber fractions that were not fabricated (for example, for 25%, 50% and 75% fiber fractions). Stress–strain results shown in Fig. 8 for different laminated composite material systems with increased fiber volume fraction. The transverse model is not presented due to similarity in fiber fraction results when the fibers were orthogonal to the loading direction.

4. Discussion

Novel bio-composite-oriented laminates, based on alginate matrix reinforced with natural collagen fibers, were fabricated and mechanically tested. Previous work [32,33] was limited to

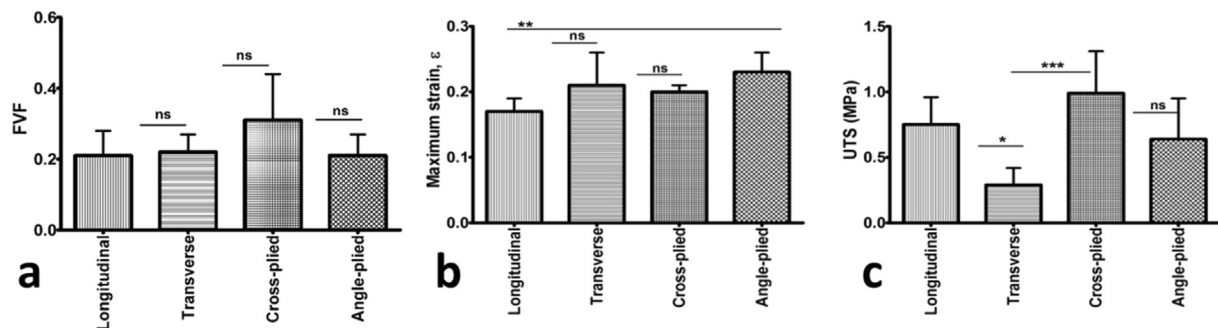


Fig. 5. Experimental values of the four bio-composites: (a) Fiber fraction of the four fabricated bio-composites measured using digital computation. (b) Ultimate tensile strain. (c) Ultimate tensile strength. (Where “*” stands for $0.01 < p \text{ value} < 0.05$, “***” $0.001 < p \text{ value} < 0.01$ and “****” $0.0001 < p \text{ value} < 0.001$).

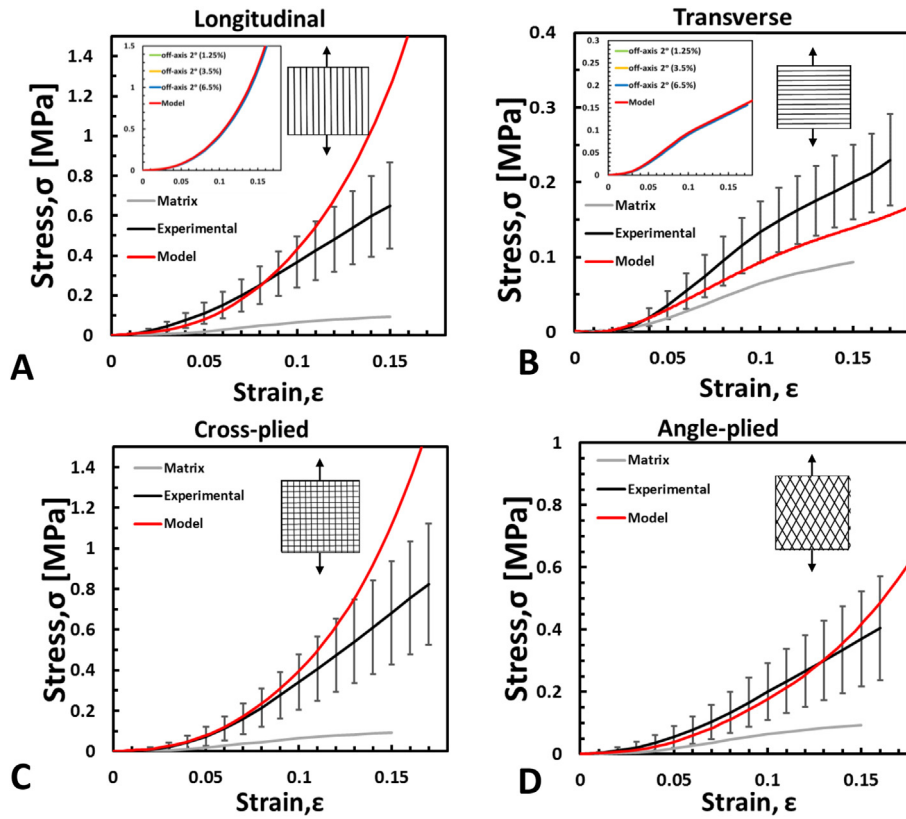


Fig. 6. Effective mechanical stress–strain behavior of the tested bio-composites compared with the corresponding FE models. (A) Longitudinal laminates. (B) Transverse laminates. The inner images present the results of FE models with 2° off axis of fibers in comparison to the model without off-axis fibers. (C) Cross-plyed laminates. (D) Angle-plyed laminates. The calibrated stress–strain curve for the matrix is plotted as a reference.

manufacturing and testing this material system in its unidirectional reinforcement. This study introduces and investigates multi-layered laminates with collagen reinforcements having different orientations. These biomimicry inspired fiber-reinforced composite systems provide a relatively simple method for tailoring their mechanical properties, specifically, by changing the volume fraction of fibers and orientations. Furthermore, these composites allowed the creation of anisotropic materials in which the mechanical properties varied with loading directions, similar to the features of many soft tissues.

The laminates in the study exhibited hyperelastic behavior with similar range as native tissues, demonstrating that a combination of

materials inspired by the natural tissue combination may produce compatible material properties. For example, the mechanical properties of the angle-plyed laminates were compatible with tissues of the aorta, which consist of 25–35% collagen fibers with a strength of 0.3–0.8 MPa [1].

As with many native soft tissues, for example, the aorta is composed of several layers: the intima, adventitia and media, each with discrete properties. The media's and adventitia's tensile strengths are about 0.4 MPa and 1.4 MPa, respectively [39]. The mean angle between fiber orientations of the adventitia is about 67° with the circumferential axis, which is equivalent to the current angle-plyed ($\pm 30^\circ$) laminates with fiber fraction of about 50%. The media's angle between fiber orientations is about 21° with the circumferential axis, exhibiting about 3 times less strength. These tissue layers can be mimicked and combined as bio-composite laminates to create a complex tailor-designed aortal structure.

Significant difference in ultimate strains was observed ($p = 0.0059$) between the longitudinal and angle-plyed samples, but not between the other groups as demonstrated in Fig. 5b. The angle-plyed laminate's failure strain was higher than the longitudinal laminate's corresponding native tissue behavior. It is possible, if designed with a different matrix material, to get higher failure strains, since the alginate matrix provided limited ability to stretch, and was where the failure occurred. In nature, soft tissue types have different fibers arrangements and preferred orientations. Tissue fiber volume fraction and structural arrangement have a major impact on mechanical behavior. For example, in tendons and ligaments, collagen fibers are arranged parallel to the loading direction, resulting in high-strength tissue with relatively low strains [1,2]. These tissues are mainly subjected to uniaxial tensile loading in the

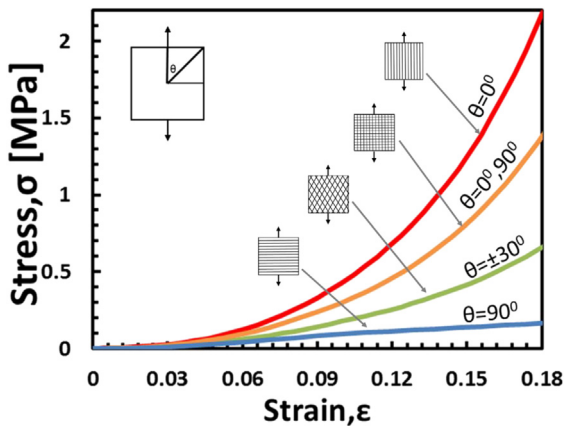


Fig. 7. Predicted stress–strain behaviors from the four FE models for FVF of 21%.

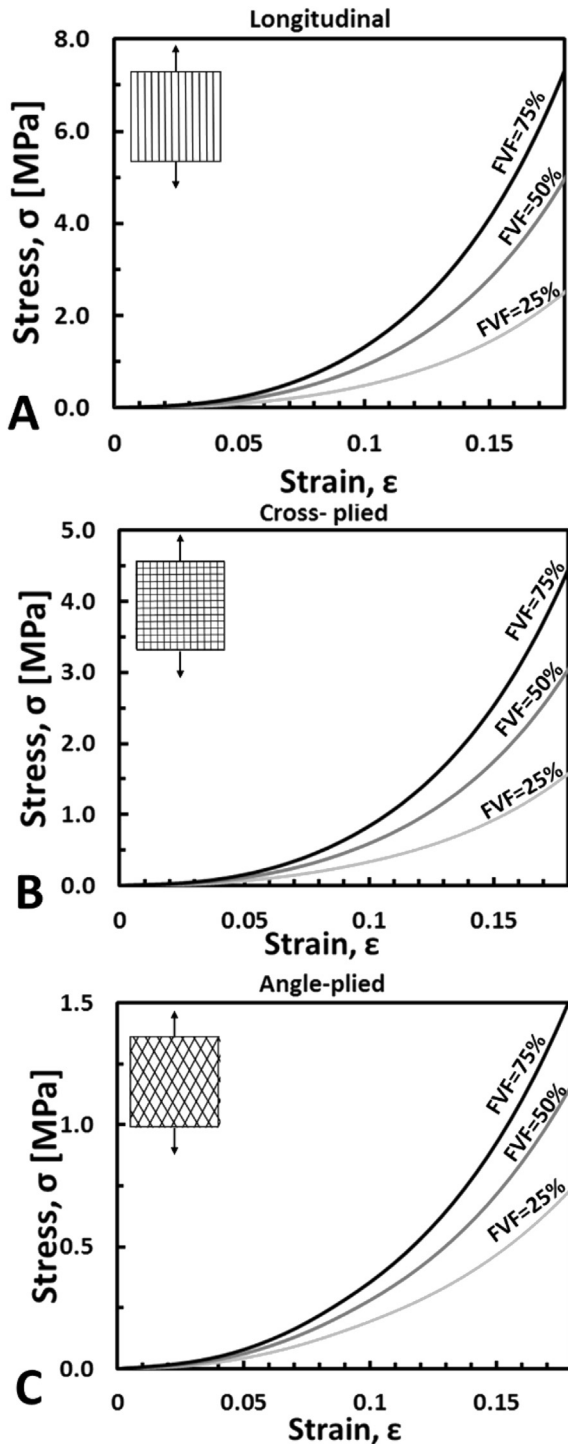


Fig. 8. Predicted effective stress–strain behaviors of bio-composite laminates having different fiber fractions. (A) Longitudinal. (B) Cross-plyed. (C) Angle-plyed.

fiber direction. In annulus fibrosus (a fibrous tissue of the intervertebral disc), which is subjected to multiaxial tension, compression and shear, for instance, fibers are arranged in $\pm 30^\circ$ lamellas. Despite its relatively low tensile strength, this tissue arrangement has the ability to withstand higher deformations [1,2]. Hence, we expected to find the same variance in ultimate strain between the angle-plyed and longitudinal laminates.

Fiber micro-crimping is characterizes soft tissues and plays a

major role in hyperelastic tissue behavior, allowing tissue durability [14,15]. The natural coral collagen coiling was preserved during the bio-composite fabrication and was verified by SEM images (Fig. 4). The method for quantifying fiber volume fraction was also verified by comparing fiber volume fraction FE model results with the corresponding experimental results.

In the fabricated samples, the fibers were aligned in preferred directions (Fig. 3), but as in natural soft tissues, some fibers were aligned off-axis. The off-axis deviation was calculated (Table 1) and a 2-degree deviation was embedded in the longitudinal and transverse FE models (Fig. 6A,B). The angle deviation had minor effect on the mechanical behavior of the composites. These finding justified the use in the models with the main direction without deviations.

The reason that the longitudinal and cross-plyed composites showed significantly higher strength compared to the transverse laminates was because in these arrangements, the collagen fibers, which were aligned in the tensile direction, bear the load. Transverse samples showed the least strength since they had no fibers in the loading direction, and most of the mechanical behavior is matrix-dominated, as seen in Fig. 7. The longitudinal and transverse laminates were actually the same samples, tested in different orientations, demonstrating anisotropic behavior: strength and stiffness were higher when load was applied in the direction parallel to the collagen fibers.

Experimental results provided mechanical information on bio-composites with fiber fractions of about 20–30%. However, these results did not provide information about the mechanical behaviors of other FVFs. Toward this goal, an FE heterogeneous micro-model was proposed to analyze and predict the mechanical behavior of the four tested material systems, and to examine other possible configurations with different FVFs. The FE model provided good predictions for mechanical response of the fabricated laminates. In the angle-plyed laminates, the predicted stress–strain curve was good throughout the entire testing range. For cross-plyed and longitudinal laminates, the predicted behavior was accurate up to about 10% strain, and then the model predicted higher stresses than the actual measurements. The reason for these results could be that additional mechanical mechanisms were playing a role, such as plastic deformations or damage behavior, which the current model did not include in the constitutive parts for the fiber and matrix constituents.

The FE model showed that the fibers carried most of the load and were able to bare higher stress levels with increased FVF (Fig. 8). Therefore, for the same level of FVF, the longitudinal laminate was stiffer than the cross-plyed laminate, which was stiffer than the angle-plyed. While the transverse laminate was the least stiff, since it had no fibers in the loading direction. However, in the transverse laminate case, the increase in FVF did not have a noticeable effect since the behavior is strongly matrix-dominated.

The models' hyperelastic material properties were based on experimental results. An alginate matrix was tested as a matrix-only material, but in-situ collagen fiber properties did not represent the fiber-alone properties due to its complex structure. Therefore, the deduced effective fiber stress–strain curve can be viewed as describing the fibers in the form of an idealized continuum with cylindrical cross-section. This can explain why the tested load-deflection of a collagen fiber bundle yielded drastically lower stress–strain curve. This is due to the fact that the bundle was a collection of discrete coiled fibers that did not act as continuous media. Moreover, the environment of the single-bundle fiber tests (wet/dry conditions) along with the internal fiber–fiber intra-slip caused the low effective mechanical response of the calibrated fibers. In addition to its role as a binder, the matrix provided an aqueous surrounding to the collagen fibers. This aqueous

surrounding allowed internal inter-fiber slipping similar to the non-collagenous component of native soft tissues [40].

The strain rate influence was examined and found to have negligible effect on the results since the overall imposed displacement rate was in the quasi-static level. Faster strain rates allowed computationally efficient modeling and rapid convergence.

The in-silico aided design, using the proposed FE models in combination with selective manufacturing of the bio-composite laminates, provide a good starting point for soft tissue mimicry of complex structures as of native tissues.

5. Limitations

The FE models included several idealizations neglecting several material complexities, such as matrix porosity, fiber coiling, and nano-to-micro level hierarchical micro-structures. The models did not account for any mechanism to simulate tissue damage. Collagen fibers were assumed to be a continuum, with a radial cross-section. Increasing fiber fraction was done by increasing the cross-section effective diameter. Temperature influence was not tested and fabrication and mechanical testing were conducted in room temperature, the collagen should not be significantly affected since its melting temperature is 68 °C [34]. Variability of the orientation exists in all manufactured composite systems. However, the mechanical response was not strongly influenced.

6. Conclusions

We have created novel collagen fiber-reinforced bio-composite laminates that exhibited overall hyperelastic behavior and biocompatible constituents, similar to native tissues. The bio-composites were fabricated in four fiber orientations and their mechanical response was tested and characterized. Hyperelastic FE anisotropic models were developed and found able to predict the overall tensile behavior as a function of the different fiber volume fractions. The mechanical behaviors were found to be in the same range of well-known native soft tissues. The calibrated model may be used as mechanical framework and provide a good starting point for soft tissue mimicry and tissue repair. More complex structures with tailored mechanical functions can be designed with the proposed model.

References

- [1] G.A. Holzapfel, *Biomechanics of Soft Tissue*, in: *Handbook of Material Behavior-non Linear Models and Properties*, Graz University of Technology, 2001.
- [2] R.L. Mauck, B.M. Baker, N.L. Nerurkar, J.A. Burdick, W.-J. Li, R.S. Tuan, et al., Engineering on the straight and narrow: the mechanics of nanofibrous assemblies for fiber-reinforced tissue regeneration, *Tissue Eng. Part B Rev.* 15 (2009) 171–193.
- [3] J.W. Ruberti, A.S. Roy, C.J. Roberts, Corneal biomechanics and biomaterials, *Annu. Rev. Biomed. Eng.* 13 (2011) 269–295, <http://dx.doi.org/10.1146/annurev-bioeng-070909-105243>.
- [4] M.S. Kunal Singha, Biomechanism profile of intervertebral disc's (IVD): strategies to successful tissue engineering for spinal healing by reinforced composite structure, *J. Tissue Sci. Eng.* 3 (2012) 1–13.
- [5] S.A. Sell, P.S. Wolfe, K. Garg, J.M. McCool, I.A. Rodriguez, G.L. Bowlin, The use of natural polymers in tissue engineering: a focus on electrospun extracellular matrix analogues, *Polymers (Basel)* 2 (2010) 522–553.
- [6] C.P. Barnes, S.A. Sell, E.D. Boland, D.G. Simpson, Nanofiber technology designing the next generation of tissue engineering scaffolds, *Adv. Drug Deliv. Rev.* 59 (2007) 1413–1433.
- [7] A. Tamayol, M. Akbari, N. Annabi, A. Paul, A. Khademhosseini, D. Juncker, Fiber-based tissue engineering: progress, challenges, and opportunities, *Bio-technol. Adv.* 31 (2013) 669–687, <http://dx.doi.org/10.1016/j.biotechadv.2012.11.007>.
- [8] P.A. Gunatillake, R. Adhikari, Biodegradable synthetic polymers for tissue engineering, *Eur. Cells Mater.* 5 (2003) 1–16.
- [9] F.T. Moutos, L.E. Freed, F. Guillek, A biomimetic three-dimensional woven composite scaffold for functional tissue engineering of cartilage, *Nat. Mater.* 6 (2007) 162–167, <http://dx.doi.org/10.1038/nmat1822>.
- [10] J.A. Cooper, J.S. Sahota, W.J. Gorum, J. Carter, S.B. Doty, C.T. Laurencin, Biomimetic tissue-engineered anterior cruciate ligament replacement, *Proc. Natl. Acad. Sci. U. S. A.* 104 (2007) 3049–3054, <http://dx.doi.org/10.1073/pnas.0608837104>.
- [11] V.A. Kumar, J.M. Caves, C.A. Haller, E. Dai, L. Liu, S. Grainger, et al., Acellular vascular grafts generated from collagen and elastin analogs, *Acta Biomater.* 9 (2013) 8067–8074.
- [12] N.L. Nerurkar, B.M. Baker, S. Sen, E.E. Wible, D.M. Elliott, R.L. Mauck, Nanofibrous biologic laminates replicate the form and function of the annulus fibrosus, *Nat. Mater.* 8 (2009) 986–992, <http://dx.doi.org/10.1038/nmat2558>.
- [13] N.L. Nerurkar, D.M. Elliott, R.L. Mauck, Mechanics of oriented electrospun nanofibrous scaffolds for annulus fibrosus tissue engineering, *J. Orthop. Res.* 25 (2007) 1018–1028, <http://dx.doi.org/10.1002/jor.20384>.
- [14] S. Fleischer, R. Feiner, A. Shapira, J. Ji, X. Sui, H. Daniel Wagner, et al., Spring-like fibers for cardiac tissue engineering, *Biomaterials* 34 (2013) 8599–8606.
- [15] J.M. Caves, V.A. Kumar, W. Xu, N. Naik, M.G. Allen, E.L. Chaikof, Microcrimped collagen fiber-elastin composites, *Adv. Mater.* 22 (2010) 2041–2044, <http://dx.doi.org/10.1002/adma.200903612>.
- [16] M. Bhattacharjee, S. Miot, A. Gorecka, K. Singha, M. Loparic, S. Dickinson, et al., Oriented lamellar silk fibrous scaffolds to drive cartilage matrix orientation: towards annulus fibrosus tissue engineering, *Acta Biomater.* 8 (2012) 3313–3325, <http://dx.doi.org/10.1016/j.actbio.2012.05.023>.
- [17] T. Courtney, M.S. Sacks, J. Stankus, J. Guan, W.R. Wagner, Design and analysis of tissue engineering scaffolds that mimic soft tissue mechanical anisotropy, *Biomaterials* 27 (2006) 3631–3638.
- [18] D. Tremblay, T. Zigras, R. Cartier, L. Leduc, J. Butany, R. Mongrain, et al., A comparison of mechanical properties of materials used in aortic arch reconstruction, *Ann. Thorac. Surg.* 88 (2009) 1484–1491.
- [19] D.I. Zeugolis, G.R. Paul, G. Attenburrow, Cross-linking of extruded collagen fibers—a biomimetic three-dimensional scaffold for tissue engineering applications, *J. Biomed. Mater. Res. Part A* 89A (2008) 895–908.
- [20] C.E. Ghezzi, B. Marelli, N. Muja, S.N. Nazhat, Immediate production of a tubular dense collagen construct with bioinspired mechanical properties, *Acta Biomater.* 8 (2012) 1813–1825.
- [21] M. Kharaziha, M. Nikkha, S.-R. Shin, N. Annabi, N. Masoumi, A.K. Gaharwar, et al., PGS: gelatin nanofibrous scaffolds with tunable mechanical and structural properties for engineering cardiac tissues, *Biomaterials* 34 (2013) 6355–6366.
- [22] L. Moroni, J.R. De Wijn, C.A. Van Blitterswijk, 3D fiber-deposited scaffolds for tissue engineering: influence of pores geometry and architecture on dynamic mechanical properties, *Biomaterials* 27 (2006) 974–985.
- [23] N.J. Amoroso, A. D'Amore, Y. Hong, C.P. Rivera, M.S. Sacks, W.R. Wagner, Microstructural manipulation of electrospun scaffolds for specific bending stiffness for heart valve tissue engineering, *Acta Biomater.* 8 (2012) 4268–4277.
- [24] J.M. Caves, W. Cui, J. Wen, V.A. Kumar, E.L. Chaikof, Elastin-like protein matrix reinforced with collagen microfibrils for soft tissue repair, *Biomaterials* 32 (2011) 5371–5379.
- [25] L.D. Wright, K.D. McKeon Fischer, Z. Cui, L.S. Nair, J.W. Freeman, PDLA/PLLA and PDLA/PCL nanofibers with a chitosan based hydrogel in composite scaffolds for tissue engineered cartilage, *J. Tissue Eng. Regen. Med.* 8 (2012) 946–954.
- [26] S. Pok, J.D. Myers, S.V. Madhally, J.G. Jacot, A multi-layered scaffold of a chitosan and gelatin hydrogel supported by a pcl core for cardiac tissue engineering, *Acta Biomater.* 9 (2013) 5630–5642.
- [27] A. Sasson, S. Patchornik, R. Eliasy, D. Robinson, R. Haj-Ali, Hyperelastic mechanical behavior of chitosan hydrogels for nucleus pulposus replacement—experimental testing and constitutive modeling, *J. Mech. Behav. Biomed. Mater.* 8 (2012) 143–153.
- [28] R.A. Neal, A. Jean, H. Park, P.B. Wu, J. Hsiao, G.C. Engelmayr Jr., et al., Three-dimensional elastomeric scaffolds designed with cardiac-mimetic structural and mechanical features, *Tissue Eng. Part A* 19 (2012) 793–807.
- [29] A.G. Mitsak, A.M. Dunn, S.J. Hollister, Mechanical characterization and non-linear elastic modeling of poly (glycerol sebacate) for soft tissue engineering, *J. Mech. Behav. Biomed. Mater.* 11 (2012) 3–15.
- [30] N.L. Nerurkar, R.L. Mauck, D.M. Elliott, Modeling interlamellar interactions in angle-ply biologic laminates for annulus fibrosus tissue engineering, *Biomech. Model. Mechanobiol.* 10 (2011) 973–984.
- [31] N.L. Nerurkar, R.L. Mauck, D.M. Elliott, ISSLS prize winner: integrating theoretical and experimental methods for functional tissue engineering of the annulus fibrosus, *Spine (Phila Pa 1976)* 33 (2008) 2691–2701, <http://dx.doi.org/10.1097/BRS.0b013e31818e61f7>.
- [32] M. Sharabi, Y. Mandelberg, D. Benayahu, Y. Benayahu, A. Azem, R. Haj-Ali, A new class of bio-composite materials of unique collagen fibers, *J. Mech. Behav. Biomed. Mater.* 36 (2014) 71–81.
- [33] Haj-Ali R, Benayahu Y, Benayahu D, Sasson-levi A, Sharabi M. WO 2013118125 A1, Composites Comprising Collagen Extracted from Sarcophyton Sp. Coral, 2013.
- [34] Benayahu Y, Kashman Y, Sela I, Raz E. US20110038914A1, Coral Derived Collagen and Methods of Farming Same, 2011.
- [35] E. Fonck, G.G. Feigl, J. Fasel, D. Sage, M. Unser, D.A. Rüfenacht, et al., Effect of aging on elastin functionality in human cerebral arteries, *Stroke* 40 (2009) 2552–2556.
- [36] R.W. Ogden, Large deformation isotropic elasticity – on the correlation of theory and experiment for incompressible rubberlike solids, *Proc. R. Soc. A*

- Math. Phys. Eng. Sci. 326 (1972) 565–584.
- [37] Abaqus theory manual. Abaqus 613 Doc, 2014.
- [38] R.S. Marlow, A General First-invariant Hyperelastic Constitutive Model, in: Constitutive Models for Rubber III, Swets & Zeitlinger, 2003.
- [39] G.A. Holzapfel, G. Sommer, C.T. Gasser, P. Regitnig, Determination of layer-specific mechanical properties of human coronary arteries with non-atherosclerotic intimal thickening and related constitutive modeling, *Am. J. Physiol. Heart Circ. Physiol.* 289 (2005) H2048–H2058.
- [40] C.T. Thorpe, H.L. Birch, P.D. Clegg, H.R.C. Screen, The role of the non-collagenous matrix in tendon function, *Int. J. Exp. Pathol.* 94 (2013) 248–259.